PREDICTION OF TIME-MEAN CHARACTERISTICS AND PERIODICAL FLUCTUATION OF VELOCITY AND THERMAL FIELDS OF A BACKWARD-FACING STEP

K. TATSUMI, H. IWAI, E. C. NEO, K. INAOKA and K. SUZUKI

Department of Mechanical Engineering, Kyoto University

Yoshida Honmachi, Sakyo-ku, Kyoto 606-8501,Japan

ABSTRACT

The present study presents the results of a three-component decomposition approach for the two- and three-dimensional computations of a turbulent flow over a backward-facing step. By this approach, effect of periodical fluctuation on the studied flow and temperature field incurred by the discrete counter-rotating vortices appearing in the free shear layer is discussed. Consequently, significance of the influence of this periodical fluctuation to the instantaneous fluid and heat transfer characteristics and eventually to the time mean momentum and heat transfer is demonstrated.

INTRODUCTION

Significant achievement has been obtained in the past decades for the turbulence modeling and numerical simulation of a variety of turbulent flows employing the proposed models. However, it is still difficult to fully predict the detailed structure of turbulent flows. It is also difficult to develop a general turbulence model applicable both for wall-bounded and free shear turbulent flows. Most of the turbulent flows include not only the turbulent fluctuation but also the large time scale fluctuation of quantities. One good example is the fluctuations of velocity and temperature fields accompanying the Kármán vortex or large-eddy structure in the shear layer. It is important to discriminate apparent shear stress and heat flux produced by these fluctuations from the one of turbulent fluctuations in order to have a correct analysis of the velocity and temperature fields. This is demonstrated in the present study through numerical computation of a turbulent flow over a backward-facing step.

Inaoka *et al.* (1998) recently showed that the dissimilarity between momentum transfer and heat transfer observed in a turbulent boundary layer disturbed with an inserted square rod can be numerically predicted with a three-component decomposition approach. With this approach, it was demonstrated that the apparent shear stress and heat flux produced by the periodical fluctuation of velocity and temperature can significantly affect the time mean momentum and heat transfer in the disturbed boundary layer. The same approach can be applied to other types of similar flows in which periodically changing velocity and temperature fields can play an important role in momentum and heat transfer. Thus, in this study, an effort has been made to apply this three-component decomposition approach to a turbulent backward-facing step flow.

Flow separation and subsequent reattachment of the separated layer are encountered in many wall flows of practical interest and significantly influence the local heat transfer characteristics. Therefore, comprehensive knowledge of detailed structure and prediction of such separated flow and accompanied heat transfer are of practical importance. One of the simplest geometry of such flows is a flow passing a backward-facing step. For this reason, large amount of experimental works and numerical calculations has been carried out in the past few decades. However, physical structure of the flow and the heat transfer processes are not yet fully understood.

In the separated shear layer, counter rotating vortices are generated. Especially in low Reynolds number range, periodical components of velocity and temperature fluctuations relating to the vortical structure contribute significantly to the momentum and heat transfer there. For example, significance of the periodical components can be seen in the location of flow reattachment point, which fluctuates back and forth in the streamwise direction. However, their effects have not been discussed in detail. For an accurate prediction of the reattaching flow, such discussion is indispensable. Therefore, in this study, time mean and periodically changing parts of velocity and temperature fields are calculated with a three-component decomposition approach for the flow over a backward-facing step. Both of 2-D and 3-D unsteady computations have been carried out in this study.

TABLE 1 : NOMENCLATURE.

HD = height of duct upstream of the step	WD = width of the duct
H = height of the step	$AR = \frac{WD}{H}$, aspect ratio
$ER = \frac{H+HD}{H}$,expansion ratio	$Re = \frac{\rho U_{ref} H}{\mu}$,Reynolds number based on step height
$Nu = \frac{q_w H}{[\lambda(T_w - T_0)]}$, mean Nusselt number	$C_f = \frac{\tau_w}{(\rho U_{ref}{}^2/2)}$, mean skin friction coefficient
τ_w = wall shear stress	q_w = wall heat flux
T_w = wall temperature	T_0 = inlet Temperature
ρ = density of air	c_p = specific heat capacity at constant pressure
λ = fluid thermal conductivity	U_{ref} = inlet freestream mean velocity
Pr_t = turbulent Prandtl number	

COMPUTATION METHOD AND PROCEDURE

Three-component decomposition approach is based on the following manipulation of the governing equations (Reynolds and Hussain, 1972). Considering the unsteadiness of flows as a superposition of slow periodical fluctuation and turbulent irregular fluctuation, all variables are decomposed into three components; namely time mean value, periodical fluctuation and turbulent fluctuation respectively. This decomposition is mathematically expressed by the following equations respectively for velocity component u_i in x_i direction, pressure p and temperature θ:

$$u_i = \bar{u_i} + \tilde{u_i} + u_i' =< u_i > + u_i' \quad (1)$$

$$p = \bar{p} + \tilde{p} + p' =< p > + p' \quad (2)$$

$$\theta = \bar{\theta} + \tilde{\theta} + \theta' =< \theta > + \theta' \quad (3)$$

where $\bar{A}$ denotes the time mean value of a quantity, $\tilde{A}$ the periodical part of the fluctuation of the quantity and A' the turbulent stochastic component of the fluctuation of the quantity. <> denotes the phase average.

The governing equation for u_i may be written as follows:

$$\frac{\partial u_i}{\partial x_i} = 0 \quad (4)$$

$$\frac{\partial u_i}{\partial t_i} + u_j \frac{\partial u_i}{\partial x_j} = -\frac{\partial p}{\partial x_i} + \frac{1}{Re}\frac{\partial^2 u_i}{\partial x_j \partial x_j} \quad (5)$$

where Re is the flow Reynolds number. Substituting Eqs.(1)-(3) into Eq.(5) taking account of Eq.(4) and operating phase average, one obtains the following equation for $< u_i >$.

$$\frac{\partial u_i}{\partial t} + < u_j > \frac{\partial < u_i >}{\partial x_j} = -\frac{\partial < p >}{\partial x_i} + \frac{1}{Re}\frac{\partial^2 < u_i >}{\partial x_j \partial x_j} - \frac{\partial}{\partial x_j} < u_i' u_j' > \quad (6)$$

The third term of the right hand side of the above equation is modeled with a non-linear turbulence model proposed by the UMIST group (Suga, 1995).

$$\begin{aligned} \rho\overline{u_i u_j} &= \frac{2}{3}k\rho\delta_{ij} - \mu_t S_{ij} \quad (7) \\ &+c_1\mu_t\frac{k}{\tilde{\varepsilon}}\left(S_{ik}S_{kj} - \frac{1}{3}S_{kl}S_{kl}\delta_{ij}\right) \\ &+c_2\mu_t\frac{k}{\tilde{\varepsilon}}\left(\Omega_{ik}S_{kj} + \Omega_{jk}S_{ki}\right) \\ &+c_3\mu_t\frac{k}{\tilde{\varepsilon}}\left(\Omega_{ik}\Omega_{jk} - \frac{1}{3}\Omega_{lk}\Omega_{lk}\delta_{ij}\right) \\ &+c_4\mu_t(\frac{k}{\tilde{\varepsilon}})^2\left(S_{ki}\Omega_{lj} + S_{kj}\Omega_{li}\right)S_{kl} \\ &+c_5\mu_t(\frac{k}{\tilde{\varepsilon}})^2\Big(\Omega_{il}\Omega_{lm}S_{mj} + S_{il}\Omega_{lm}\Omega_{mj} \\ &\quad - \frac{2}{3}S_{lm}\Omega_{mn}\Omega_{nl}\delta_{ij}\Big) \\ &+c_6\mu_t(\frac{k}{\tilde{\varepsilon}})^2 S_{ij}S_{kl}S_{kl} \\ &+c_7\mu_t(\frac{k}{\tilde{\varepsilon}})^2\Omega_{ki}\Omega_{kj}\Omega_{kl} \end{aligned}$$

where

$$S_{ij} = \left(\frac{\partial U_i}{\partial x_j} + \frac{\partial U_j}{\partial x_i}\right), \quad \Omega_{ij} = \left(\frac{\partial U_i}{\partial x_j} - \frac{\partial U_j}{\partial x_i}\right)$$

$$\tilde{S} = \frac{k}{\tilde{\varepsilon}}\sqrt{S_{ij}S_{ij}/2}, \quad \tilde{\Omega} = \frac{k}{\tilde{\varepsilon}}\sqrt{\Omega_{ij}\Omega_{ij}/2}$$

$$\mu_t = \rho C_\mu f_\mu \frac{k^2}{\tilde{\varepsilon}}$$

Similarly, energy equation in terms of $< \theta >$ can be expressed as follows:

$$\frac{\partial \theta}{\partial t} + < u_j > \frac{\partial < \theta >}{\partial x_j} = \frac{1}{RePr}\frac{\partial^2 < \theta >}{\partial x_j \partial x_j} - \frac{\partial}{\partial x_j} < u_i'\theta' > \quad (8)$$

$$- < u_i'\theta' > = \frac{\nu_t}{Pr_t}\frac{\partial < \theta >}{\partial x_i} \quad (9)$$

Turbulent Prandtl number was assumed to be constant in this study and was taken to be $Pr_t = 0.9$.

The computational domain in the present computations is illustrated in Fig. 1 with the coordinate system to be used. The origin of the coordinate system is located at the center of the bottom corner of the step.

The 3-D simulations performed in the present work were carried out under conditions close to those studied by Papadopoulos *et al.* (1995). The expansion ratio was set to be $ER = 2$ for 3-D computation and $ER = 1.2$ for 2-D computation. The aspect ratio in 3-D computation was set to be $AR = 4$. The boundary layer thickness at the inlet was $\delta/H \approx 0.16$. 5,200 was chosen for the Reynolds number in the present study while the flow studied by Papadopoulos *et al.* was at the Reynolds number 26,500. This was to decrease the grid number so as to complete calculation within a reasonable computation time. For boundary conditions at walls, all variables except temperature were set equal to zero. For the thermal

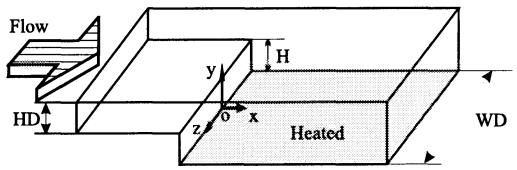

Figure 1 Computational domain.

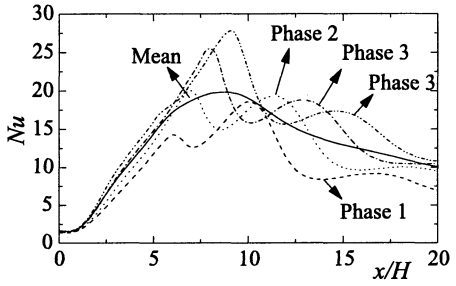

Figure 2 Instantaneous Nusselt number at different phases. (2-D)

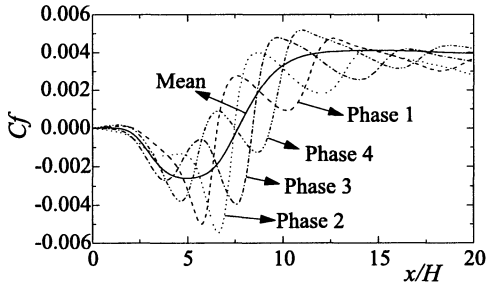

Figure 3 Instantaneous skin friction coefficient at different phases. (2-D)

boundary conditions, the bottom wall downstream of the step was set to be heated at a constant heat flux and other walls were treated as adiabatic.

RESULTS AND DISCUSSION

First the results of the 2-D computation will be discussed. Instantaneous Nusselt number and skin friction coefficient distributions at different phases are shown in Fig. 2 and Fig. 3 together with their time mean values. Both values noticeably vary from one phase to another. This is due to the unsteadiness of the flow related to the periodic formation of vortex in the separated shear layer. Comparing the two figures, at some positions, peak instantaneous Nusselt number is found to appear around the dent in the distribution of skin friction coefficient. This indicates the generation of the instantaneous dissimilarity between the heat transfer and momentum transfer as in the case of the turbulent boundary layer disturbed by an inserted cylinder (Inaoka et al., 1998, 1999). The locations of the reattachment point for each time phases are tabulated in Table 2. The reattachment point is defined as the first point from the step at which the skin friction coefficient

TABLE 2 : REATTACHMENT POINTS.

	2-D ($ER = 1.2$)	3-D ($ER = 2$)
Phase 1	$5.90H$	$8.12H$
Phase 2	$7.47H$	$8.50H$
Phase 3	$8.41H$	$8.13H$
Phase 4	$5.94H$	$8.53H$
Mean	$7.60H$	$8.54H$

changes its sign from negative to positive. The locations vary by large amount moving back and forth centering the mean value.

Figure 4 illustrates the spatial distributions both of an apparent wall-normal heat flux produced by the periodical fluctuations of velocity and temperature $\tilde{v}\tilde{\theta}$ and another apparent heat flux produced by the stochastic fluctuations of velocity and temperature $< v'\theta' >$ at four different phases. $\tilde{v}\tilde{\theta}$ is calculated automatically as a part of the convection term of Eq.(8) while $< v'\theta' >$ is calculated through the model of Eq.(9) in the present computation. In this figure, the shaded parts correspond to the regions where the plotted quantities take positive value while the unshaded parts to those where they take negative value. Deeper gray color corresponds to larger heat flux. Comparing the values of both quantities, $< v'\theta' >$ is larger than $\tilde{v}\tilde{\theta}$ on the whole. However, the positions of the positive peaks of apparent heat flux due to the periodical fluctuations match the positions of the maximum peaks of the Nusselt number at every phase. This reveals that periodical fluctuation contributes to the overall heat transfer significantly.

Figure 5 shows the spatial distributions both of an apparent wall-normal Reynolds shear stress produced by the periodical velocity fluctuations, $-\tilde{u}\tilde{v}$, and another apparent Reynolds shear stress produced by the stochastic velocity fluctuations, $- < u'v' >$, in the same manner as seen in Fig. 4. In this figure, again the shaded parts correspond to the regions where the plotted quantities take positive value and unshaded parts to those of negative value. As in the case of the apparent heat flux just discussed, stochastic part of apparent shear stress takes larger value than the periodical fluctuation counterpart. However, the position of the minimum peaks of $-\tilde{u}\tilde{v}$ matches the location of the minimum values of instantaneous wall skin friction coefficient. Combining all the results discussed in the above, one can say that the intensification of the apparent heat flux contributed from $\tilde{v}\tilde{\theta}$ and the suppression of the apparent shear stress caused by the contribution from $-\tilde{u}\tilde{v}$ produces the instantaneous dissimilarity between heat transfer and momentum transfer.

Next, the results obtained from a 3-D computation will be discussed. Instantaneous Nusselt number and skin friction coefficient obtained along the centerline at different phases are shown in Fig. 6 and Fig. 7 together with their mean values. First, as in the 2-D computation, instantaneous and time mean dissimilarity appears in some regions where

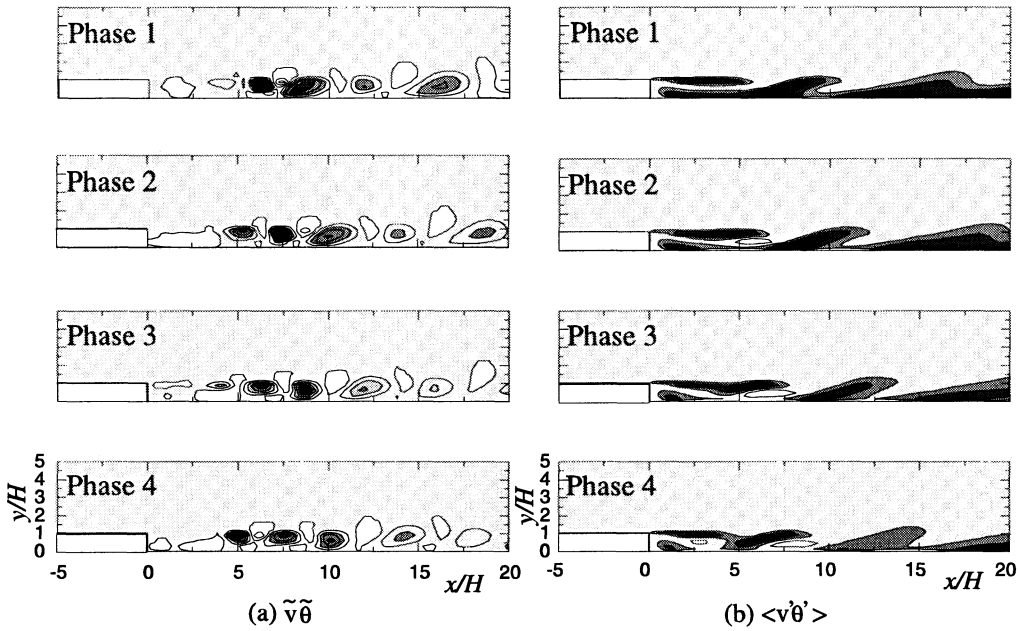

Figure 4 Instantaneous maps of apparent heat flux contours,
(a) $\tilde{v}\tilde{\theta}$ and (b) $< v'\theta' >$ (Shaded parts: positive value). (2-D)

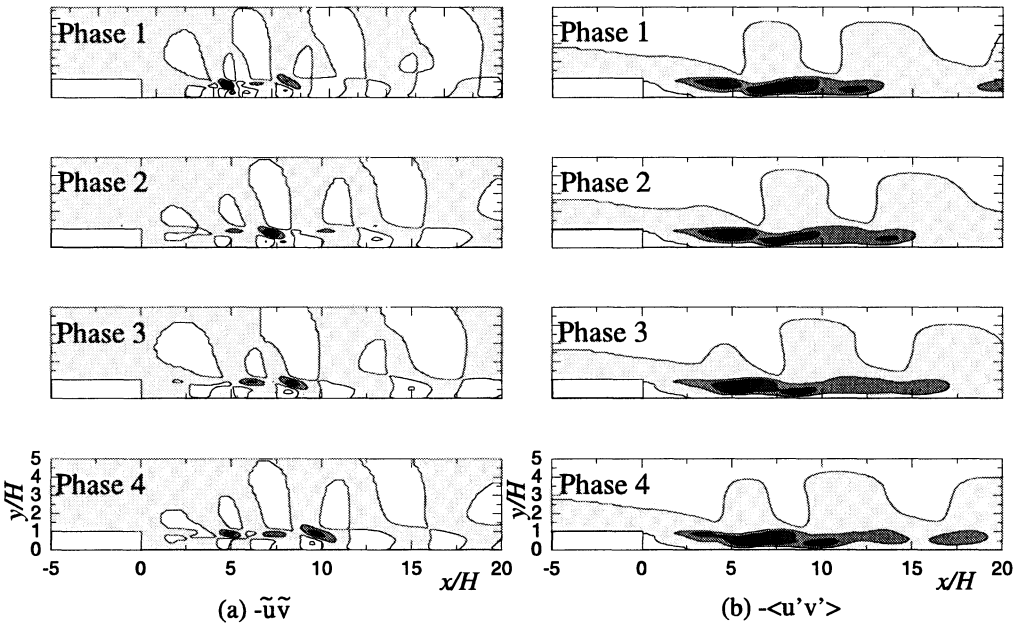

Figure 5 Instantaneous maps of apparent shear stress contours,
(a) $-\tilde{u}\tilde{v}$ and (b) $- < u'v' >$ (Shaded parts: positive value). (2-D)

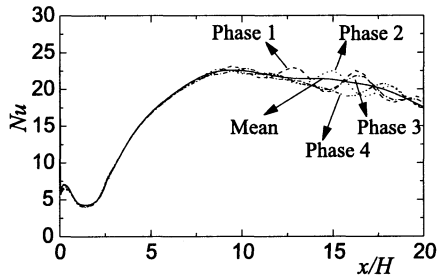

Figure 6 Instantaneous Nusselt number at different phases. (3-D, $z = 0$)

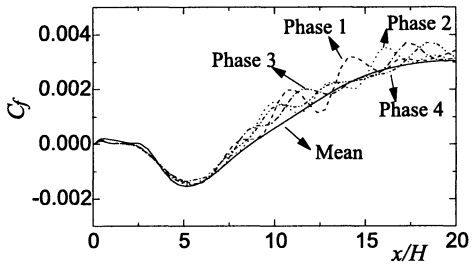

Figure 7 Instantaneous skin friction coefficient at different phases. (3-D, $z = 0$)

heat transfer increases while skin friction coefficient decreases. Comparing the results of 3-D computation with the 2-D counterparts discussed above, the plotted fluctuations in these figures are smaller. However, still a large variation from one phase to another is observed especially downstream the reattachment point. The reattachment location is tabulated in Table 2. Here also, the location shifts as the phase changes. However, comparing with the 2-D counterparts, the variations of the movements of the location are smaller.

In Fig. 8 are plotted the streamwise distributions along the centerline of wall-normal apparent heat fluxes obtained at several different phases. $\tilde{v}\tilde{\theta}$ and $< v'\theta' >$ are produced by the periodical and stochastic fluctuations of velocity and temperature fields respectively. Comparing the two quantities $< v'\theta' >$ and $\tilde{v}\tilde{\theta}$ with each other, $< v'\theta' >$ takes a larger value than $\tilde{v}\tilde{\theta}$. This is qualitatively the same as the results of the 2-D computation. Just as in the 2-D computation, the locations of the maximum peaks of instantaneous Nu number plotted in Fig. 6 match well the locations where $\tilde{v}\tilde{\theta}$ shows maximum peaks.

Figure 9 illustrates the spatial distributions along the centerline of the apparent wall normal Reynolds shear stresses, $-\tilde{u}\tilde{v}$ and $- < u'v' >$ calculated at several different phases. Comparing with the above-discussed results of 2-D computation illustrated in Fig. 5, influence of the periodical fluctuations is somewhat less pronounced in the case of 3-D computation. However, just as discussed in the 2-D results, the quantity $- < u'v' >$ shows a larger value comparing to the quantity $-\tilde{u}\tilde{v}$. The location where $-\tilde{u}\tilde{v}$ shows a minimum peak matches also well to the location where the skin friction coefficient shows its minimum peak. Additionally, increase of $\tilde{v}\tilde{\theta}$ is found at the location where the increase of the Nusselt number is observed and decrease of the apparent $-\tilde{u}\tilde{v}$ at the location where decrease of skin friction coefficient is observed. Thus, significant effect of the periodical fluctuations on the over-all characteristics of flow and thermal fields has been confirmed also in the 3-D computation.

CONCLUSION

A three-component decomposition approach was applied both in the 2- and 3-D computations for a flow over a backward-facing step in order to discuss the contribution of the periodical fluctuations and the stochastic fluctuations to the over-all characteristics of the flow and thermal fields. It is demonstrated that the periodical fluctuation seriously affects the characteristics of instantaneous flow and thermal fields. Effects of periodical components are more pronounced both at locations downstream the reattachment point and inside the recirculating flow region. Stochastic fluctuation term shows a larger contribution than the periodical term even at the Reynolds number 5,200. However, the periodical fluctuation still seriously affects the characteristics of both flow and temperature fields. Consequently, apparent shear stress and heat flux produced by the periodical fluctuation of velocity and temperature significantly affect the time mean characteristics of momentum and heat transfer.

REFERENCES

Inaoka, K., Yamamoto, J., and Suzuki, K., "Dissimilarity between heat transfer and momentum transfer in a disturbed turbulent boundary layer with insertion of a rod", *Proc. Int. Conf. in Turbulent Heat Transfer 2*, Vol.1, pp. 4-3-4-14, May 31-June 5 1998.

Inaoka, K., Yamamoto, J., and Suzuki, K., "Dissimilarity between heat transfer and momentum transfer in a disturbed turbulent boundary layer with insertion of a rod - modeling and numerical simulation -", *Int. J. Heat and Fluid Flow*, 1999. (in printing)

Papadopoulos, G., Ötügen, M. V., "Separating and Reattaching Flow Structure in a Suddenly Expanding Rectangular Duct", *Journal of Fluids Engineering*, Vol.117, pp. 17-23, 1995.

Reynolds, W.C., and Hussain, A.K.M.F., "The mechanics of an organized wave in turbulent shear flow, Part 3: Theoretical models and comparisons with experiments", *J. Fluid Mechanics*, 54-2, 263-288, 1972.

Suga, K., "Development and application of a nonlinear eddy viscosity model sensitised to stress and strain invariants", UMIST, Dept of Mechanical Engineering, Report TFD/95/11, 1995.

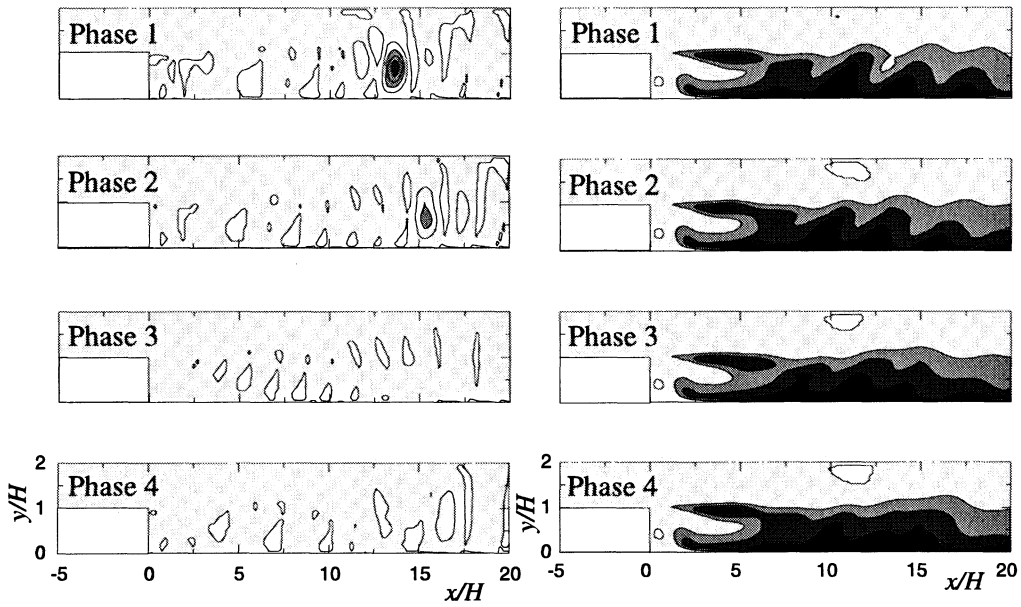

Figure 8 Instantaneous maps of apparent heat flux contours,
(a) $\tilde{v}\tilde{\theta}$ and (b) $< v'\theta' >$ (Shaded parts: positive value). (3-D, $z = 0$)

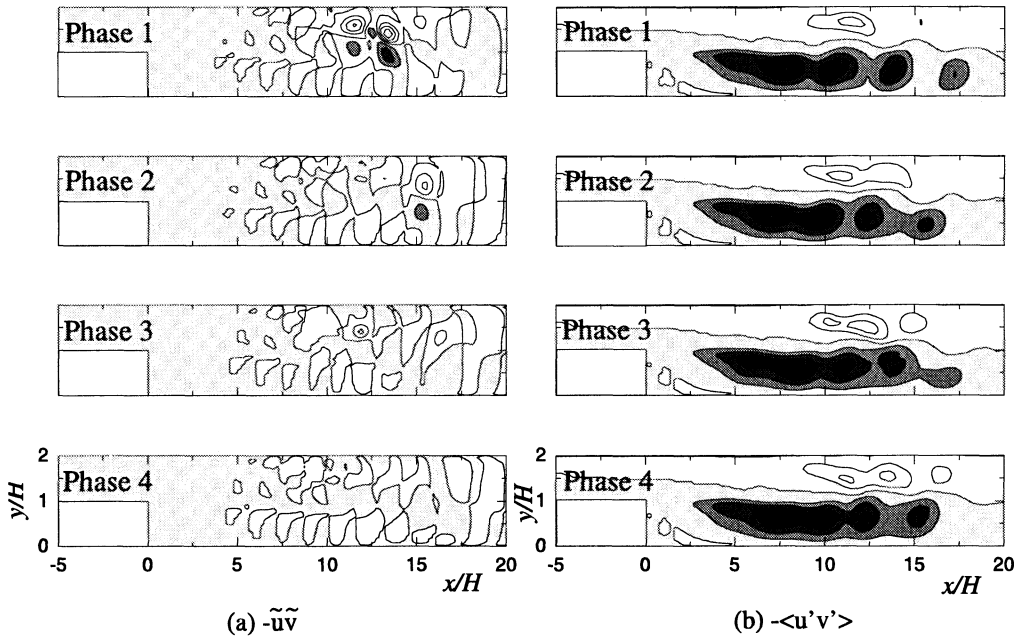

Figure 9 Instantaneous maps of apparent shear stress contours,
(a) $-\tilde{u}\tilde{v}$ and (b) $- < u'v' >$ (Shaded parts: positive value). (3-D, $z = 0$)